ISBN: 978-3-95450-179-3 doi:10.18429/JACoW-FEL2017-TUP035

CSR WAKE FIELDS AND EMITTANCE GROWTH WITH A DISCONTINUOUS GALERKIN TIME DOMAIN METHOD*

D. A. Bizzozero†, H. De Gersem, E. Gjonaj
Institut für Theorie Elektromagnetischer Felder, TU Darmstadt, Germany

Abstract

Coherent synchrotron radiation (CSR) is an essential consideration in modern accelerators and related electromagnetic structures. We present our current method to examine CSR in the time domain. The method uses a 2D Discontinuous Galerkin (DG) discretization in the longitudinal and transverse coordinates (z,x) with a Fourier decomposition in the transverse coordinate y. After summation over modes, this treatment describes all electromagnetic field components at each space-time coordinate (z,x,y,t). Additionally, by alignment of mesh element interfaces along a source reference orbit, DG methods can handle discontinuous or thin sources in the transverse x direction. We present an overview of our method, illustrate it by calculating wake functions for a bunch compressor, and discuss a method for estimating emittance growth from the wake fields in future work.

PROBLEM STATEMENT

In a continuation of earlier work [1–3], we examine the generation of CSR by an ultra-relativistic electron bunch in a vacuum chamber of rectangular cross-section. For a simplified model, we only consider motion of the bunch in a planar orbit with Cartesian coordinates (Z, X, Y) in the midplane $Y = 0$. Additionally, we only model vacuum chambers with planar horizontal boundaries at $Y = \pm h/2$ where h is the height of the chamber and only consider perfectly electrically conducting (PEC) boundary conditions on the chamber walls. An example of a chamber with a planar orbit is shown in Figure 1 (top), corresponding to the bunch compressor DESY BC0.

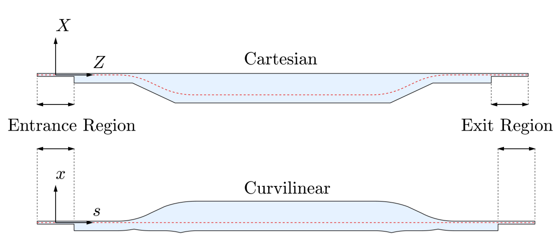

Figure 1: DESY BC0 vacuum chamber domain in (Z, X) (top) or (s, x) (bottom) coordinates with reference orbit (red dashed). The entrance region is the same in both systems.

To study CSR wake fields, we seek to time-evolve the Maxwell field equations for $\mathbf{E}$ and $\mathbf{H}$ inside the chamber:

$$\frac{\partial \mathbf{E}}{\partial \tau} = Z_0 \nabla \times \mathbf{H} - Z_0 \mathbf{j}, \qquad \frac{\partial \mathbf{H}}{\partial \tau} = -\frac{1}{Z_0} \nabla \times \mathbf{E}, \tag{1}$$

where $\tau = ct$, with speed of light c, vacuum impedance Z_0, and current density $\mathbf{j}$.

Given a smooth reference orbit parametrized by its arc length $\mathbf{R}_r(s) = (Z_r(s), X_r(s), 0)$, we transform the (Z, X, Y) coordinate system to a curvilinear system (s, x, y) with the inverse transformation of:

$$\begin{aligned} Z(s, x, y) &= Z_r(s) - x X_r'(s), \\ X(s, x, y) &= X_r(s) + x Z_r'(s), \\ \text{and } Y(s, x, y) &= y, \end{aligned} \tag{2}$$

using the signed curvature: $\kappa(s) = Z_r''(s) X_r'(s) - Z_r'(s) X_r''(s)$ and length scale factor: $\eta(s, x) = 1 + x\kappa(s)$. In the (s, x, y) coordinate system, the reference orbit is the straight line $(x, y) = (0, 0)$. Furthermore, this coordinate mapping is well-defined if $\eta > 0$ throughout the domain; where the transformation is unique. See Figure 1 (bottom) for a depiction of the curvilinear transformation of the geometry in the case of DESY BC0.

In the (s, x, y) coordinate frame, we assume a current density of the form: $\mathbf{j} = (qc\lambda(s - \tau)\delta(x)G(y), 0, 0)$ with Gaussian longitudinal and transverse distributions λ and G, and a Dirac distribution in the x-coordinate. We choose σ_s, the bunch length, such that the bunch is supported only in the entrance region to machine precision at $\tau = 0$.

We now use the parallel plate geometry of $y = \pm h/2$ to introduce a Fourier decomposition in y for all fields:

$$\begin{aligned} f(s, x, y, \tau) &= \sum_{p=1}^{\infty} f_p(s, x, \tau)\phi\big(\alpha_p(y + h/2)\big) \\ \text{and } f_p(s, x, \tau) &= \frac{2}{h}\int_{-h/2}^{h/2} f(s, x, y, \tau)\phi\big(\alpha_p(y + h/2)\big)\,dy, \end{aligned} \tag{3}$$

with $\alpha_p = \pi p/h$, f representing $E_s, E_x, E_y, H_s, H_x, H_y$ or G, and $\phi(\cdot)$ is $\sin(\cdot)$ for E_s, E_x, H_y, G or $\cos(\cdot)$ for E_y, H_s, H_x. If the initial fields and $G(y)$ are symmetric about $y = 0$, then the even p modes for all fields vanish. We denote the Fourier series modes with the subscript p.

To numerically treat the singularity at $x = 0$ in the current $\mathbf{j}$ term on the right-hand-side of (1), we apply an additional transformation on the H_{yp} field component: $\widetilde{H}_{yp} = H_{yp} - qcG_p\lambda(s - \tau)\Theta(x)$ where $\Theta(x)$ is the Heaviside function. Additional transformations can be made to transform the source to arbitrary degree of smoothness [4]; however, for a DG method with element edges which align along the discontinuity, this is not required.

Applying the curvilinear coordinate transformation in (2), the Fourier series decomposition in (3), and the transforma-

* Work supported by DESY.
† bizzozero@temf.tu-darmstadt.de

ISBN: 978-3-95450-179-3 doi:10.18429/JACoW-FEL2017-TUP035

tion for H_{yp}, to (1) yields:

$$\frac{1}{Z_0}\frac{\partial E_{sp}}{\partial \tau} = \frac{\partial \widetilde{H}_{yp}}{\partial x} + \alpha_p H_{xp}, \tag{4a}$$

$$\frac{1}{Z_0}\frac{\partial E_{xp}}{\partial \tau} = -\alpha_p H_{sp} - \frac{1}{\eta}\frac{\partial \widetilde{H}_{yp}}{\partial s} + S_E, \tag{4b}$$

$$\frac{1}{Z_0}\frac{\partial E_{yp}}{\partial \tau} = \frac{1}{\eta}\frac{\partial H_{xp}}{\partial s} - \frac{\partial H_{sp}}{\partial x} - \frac{\kappa}{\eta}H_{sp}, \tag{4c}$$

$$Z_0\frac{\partial H_{sp}}{\partial \tau} = \alpha_p E_{xp} - \frac{\partial E_{yp}}{\partial x}, \tag{4d}$$

$$Z_0\frac{\partial H_{xp}}{\partial \tau} = \frac{1}{\eta}\frac{\partial E_{yp}}{\partial s} - \alpha_p E_{sp}, \tag{4e}$$

$$Z_0\frac{\partial \widetilde{H}_{yp}}{\partial \tau} = \frac{\partial E_{sp}}{\partial x} + \frac{\kappa}{\eta}E_{sp} - \frac{1}{\eta}\frac{\partial E_{xp}}{\partial s} + S_H, \tag{4f}$$

where the source terms $S_E = -qcG_p\lambda'(s-\tau)\Theta(x)/\eta(s,x)$ and $S_H = qZ_0cG_p\lambda'(s-\tau)\Theta(x)$ arise from $\mathbf{j}$ after the H_{yp} transformation.

To initialize the time-evolution of the system in (4) we consider all fields inside the vacuum chamber to be zero initially except for the entrance region. In this region, where the reference orbit is a straight line in (Z, X, Y) with $\kappa = 0$, $\eta = 1$; the solution for a centered beam about $x = 0$ with entrance region chamber width $2d$ satisfying the PEC boundary conditions is given by:

$$\begin{aligned} E_{sp0} &= 0, & H_{sp0} &= 0,\\ E_{xp0} &= -qZ_0cG_p\lambda(s)\Phi_p(x), & H_{xp0} &= -E_{yp0}/Z_0,\\ E_{yp0} &= -qZ_0cG_p\lambda(s)\Psi_p(x), & H_{yp0} &= E_{xp0}/Z_0, \end{aligned} \tag{5}$$

and

$$\Phi_p(x) = \frac{\sinh(\alpha_p d)}{\sinh(2\alpha_p d)}\cosh\left(\alpha_p(x+d)\right) - \cosh(\alpha_p x)\Theta(x),$$

$$\Psi_p(x) = \frac{\sinh(\alpha_p d)}{\sinh(2\alpha_p d)}\sinh\left(\alpha_p(x+d)\right) - \sinh(\alpha_p x)\Theta(x).$$

However, in implementation, we use a numerical DG Poisson solver in computing the initial fields on the mesh to reduce parasitic charge effects. Lastly, the beam pipes in the entrance and exit regions are also enclosed with PEC conditions since the simulation is set to halt once the electron bunch reaches midway into the exit region of the chamber. If longer wake field simulations are desired, this exit region may be extended with little additional computational effort since the cross-sectional width is small.

DISCONTINUOUS GALERKIN METHOD

In this section we briefly outline the DG scheme used for our time-evolution of (4). Our approach follows the nodal DG foundation given in [5]. To begin, we partition the vacuum chamber domain in (s, x) into K triangular elements, with curved elements along the boundary as needed. Additionally, we impose that the reference orbit $x = 0$ lies strictly along interfaces of elements and does not bisect any element.

For a given element D^k, for $k \in \{1, ..., K\}$, we approximate each field by sums of Lagrange polynomials of Nth order denoted by $\ell_j^k(s,x)$ with $N_p = (N+1)(N+2)/2$ nodes: (s_i^k, x_i^k) where $\ell_j^k(s_i^k, x_i^k) = \delta_{ij}$, for $i, j \in \{1, ..., N_p\}$. For a field component u on element D^k, its polynomial approximation is given by:

$$u^k(s,x,\tau) = \sum_{i=1}^{N_p} u_i^k(\tau)\ell_i^k(s,x). \tag{6}$$

We next construct residuals $\mathcal{R}^k$ for each of the fields u^k from (4) which each have the form:

$$\mathcal{R}^k(s,x,\tau) = \frac{\partial u^k}{\partial \tau} - a\frac{\partial v^k}{\partial s} - b\frac{\partial w^k}{\partial x} - cw^k - f. \tag{7}$$

For example, for equation (4c): $u = E_{yp}$, $v = \widetilde{H}_{xp}$, $w = H_{sp}$, $a = Z_0/\eta$, $b = -Z_0$, $c = -Z_0\kappa/\eta$, and $f = 0$. For a Galerkin scheme, we require the residuals to be orthogonal to the same polynomial space spanned by ℓ_j^k on the element. However, a numerical flux must be introduced to couple the elements together along their edges. This flux term is a single-valued function depending on interior and exterior values along the interface. We choose an upwind flux for our hyperbolic system of equations (4). A thorough derivation of the resulting system of discrete equations is given in [2] with DG constructions detailed in [5].

With the discrete DG equations for (4) combined over all K elements, we obtain a system of $6N_pK$ equations. We evolve these equations in τ with a fourth-order low-storage explicit Runge-Kutta scheme [6].

WAKE FIELDS AND POST PROCESSING

We present simulation results for computing the longitudinal wake field by integrating E_s along the reference orbit. We define the longitudinal wake function on the orbit by:

$$\begin{aligned} w_s(z) &= \frac{-1}{q}\int_0^T E_s(\tau - z, 0, 0, \tau)d\tau \\ &= \frac{-1}{q}\sum_{p=1}^{p_{\max}}\sin\left(\frac{\pi p}{2}\right)\int_0^T E_{sp}(\tau - z, 0, \tau)d\tau. \end{aligned} \tag{8}$$

We denote z as the distance with respect to the center of the bunch along the reference orbit, not the Cartesian coordinate Z. Evaluation of E_{sp} is done while time-stepping (4) by averaging the field along $x = 0$ using the elements' DG Nth-order polynomial representation as in (6). We set T/c to be the time when the bunch is midway into the exit region.

For the transverse wake function $w_x(z)$, we replace E_s by $(E_x - Z_0H_y)$ and for the wake function $w_y(z)$ we replace E_s by $(E_y + Z_0H_x)$ in equation (8).

We also define the loss factor by:

$$L = -\int_{-\infty}^{\infty} w_s(z)\lambda(z)dz. \tag{9}$$

ISBN: 978-3-95450-179-3 doi:10.18429/JACoW-FEL2017-TUP035

In our first example, we consider a straight orbit such that $(s,x) = (Z,X)$ where the bunch passes through a rectangular beam taper. While no CSR is generated, the narrowing width of the chamber generates a longitudinal wake in Figure 2. This test is used to compare wake fields to CST Particle Studio™ [7] and PBCI [8]. The discrepancy in wake functions behind the bunch at $z \approx -50$mm is due to the difference in wake function integration methods, and diminishes as T increases. The loss factor relative error between our DG method and CST is $|L_{\mathrm{DG}} - L_{\mathrm{CST}}|/|L_{\mathrm{CST}}| = 7.87 \times 10^{-5}$.

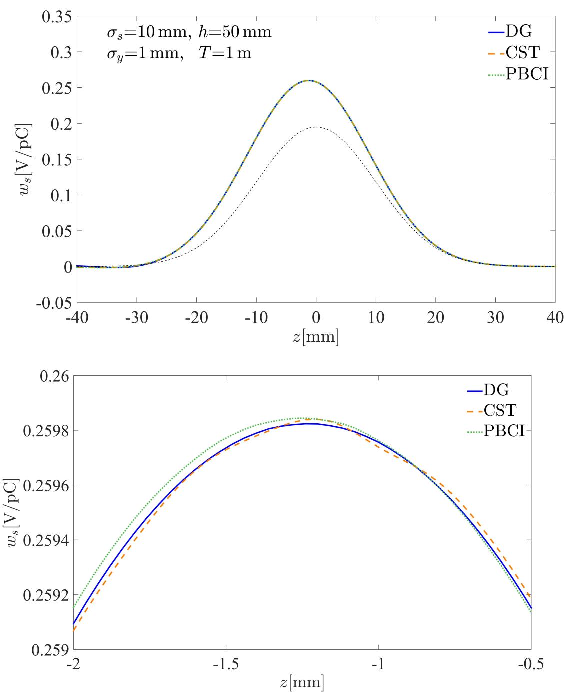

Figure 2: (Top) Wake function $w_s(z)$ shown using $N = 8$, $K = 27544$, and $p = 1, 3, 5$ modes for the tapered rectangular beam transition using our DG method, CST Particle Studio™, and PBCI. (Bottom) An enlarged view of $w_s(z)$ near $z = 0$. The thin dashed line shows the bunch profile $\lambda(z)$ scaled to the figure. The loss factor is $L = -1.847 \times 10^{-1}$ V/pC.

In our second example, we use the full DESY BC0 geometry as shown in Figure 1. In Figure 3, we plot the longitudinal wake generated by CSR and the geometry after the bunch travels along the chicane orbit comprised of straights and arcs of circles with constant curvature $\kappa = 1\,\mathrm{m}^{-1}$.

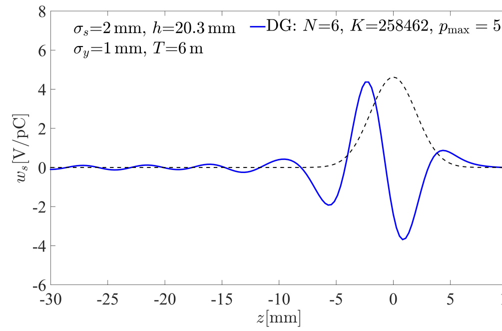

Figure 3: Wake function $w_s(z)$ for the DESY BC0 vacuum chamber. The thin dashed line shows the bunch profile $\lambda(z)$ scaled to $w_s(z)$. The loss factor is $L = 1.485 \times 10^{-5}$ V/pC.

CONCLUSION AND FUTURE WORK

In this study, we computed CSR fields generated in a bunch compressor vacuum chamber using DG finite elements in the time domain. We also presented a method to compute the longitudinal wake field and loss factors.

Our next application of this DG method will study the evolution of particle distributions by importing field maps into a particle tracking code to study emittance growth. Additionally, we will investigate the use of the Panofsky-Wenzel theorem [9] in curvilinear coordinates as an alternative approach to obtaining the transverse wake functions. We also will compare our results to paraxial frequency-domain methods [10] and other CSR codes such as CSRtrack [11].

REFERENCES

[1] D. A. Bizzozero, H. De. Gersem, and E. Gjonaj, "Coherent Synchrotron Radiation and Wake Fields With Discontinuous Galerkin Time Domain Methods", in *Proceedings of IPAC 2017*, Copenhagen, Denmark, May 2017.

[2] D. A. Bizzozero, *Studies of Coherent Synchrotron Radiation with the Discontinuous Galerkin Method*, Ph.D. Dissertation, Applied Math, University of New Mexico, 2015.

[3] B. E. Billinghurst et al., "Observation of Wakefields and Resonances in Coherent Synchrotron Radiation", *Phys. Rev. Lett.* 114, 204801, 2015.

[4] R. L. Warnock and D. A. Bizzozero, "Efficient Computation of Coherent Synchrotron Radiation in a Rectangular Chamber", *Phys. Rev. Accel. Beams* **19**, 090705, 2016.

[5] J. Hesthaven and T. Warburton, *Nodal Discontinuous Galerkin Methods* New York: Springer, 2008.

[6] J. C. Butcher, *The Numerical Analysis of Ordinary Differential Equations: Runge-Kutta and General Linear Methods*, New York: Wiley & Sons, 2003.

[7] CST AG (2016), Bad Nauheimer Str. 19, 64289 Darmstadt, Germany. Retrieved from http://www.cst.com.

[8] E. Gjonaj, T. Lau, S. Schnepp, F. Wolfheimer, and T. Weiland, "Accurate Modelling of Charged Particle Beams in Linear Accelerators", *New J. Phys.* Vol 8, November 2006.

[9] W. K. H. Panofsky and W. A. Wenzel "Some Considerations Concerning the Transverse Deflection of Charged Particles in Radio-Frequency Fields", *Rev. Sci. Instrum.* **27**, pp. 967, 1956.

[10] D. Zhou, K. Ohmi, K. Oide, L. Zang, and G. Stupakov, "Calculation of Coherent Synchrotron Radiation Impedance for a Beam Moving in a Curved Trajectory", *Jpn. J. Appl. Phys.* 51, 016401, 2012.

[11] M. Dohlus and T. Limberg, "CSRtrack: Faster Calculation of 3-D CSR Effects", in *Proceedings of FEL 2004*, Trieste, Italy, August 2004.